FSO Path Loss Model Based on the Visibility

R. Nebuloni and E. Verdugo

***Abstract*—Free-space optics (FSO) is attracting renewed attention in the frame of 5G, which demands wireless backhauling technologies with extremely high data rates over distances up to a few kilometers. Link availability is a FSO well-known issue due to the large path loss expected during poor visibility, such as in case of fog. Several path loss models, based on the visibility, are assessed through an analytical approach. The simple relationship valid in the visible spectrum can be extended to the first optical window, while, at 1.550 μm, the effect of fog microphysics cannot be ignored. Fog is definitively less challenging in the mid-IR (10.6 μm) even at very low visibility values (less than 0.5 km), which was not evident from older studies. Lower and upper bounds for the extinction coefficient are calculated and substituted into the FSO link budget equation. The combined effect of the microphysics and of the accuracy of visibility measurements may result in large uncertainties on the maximum achievable path length. The latter is also influenced by the microclimate, as links are usually deployed in urban areas while visibility data are collected outside. Path lengths in city areas can double, for the same link availability.**

***Index Terms*—Optical communication, free-space optics, visibility, fog, attenuation, extinction coefficient, mid-IR, near-IR, path loss.**

I. Introduction

FREE Space Optics (FSO) is a wireless communication technology relying on the transmission of modulated optical beams. FSO usually refers to terrestrial point-to-point links in an outdoor environment [1]. Despite the research on this topic has been active since several decades, practical applications in the telecommunication area have been restricted to niche markets as temporary or back-up links (e.g., for emergency recovery), wireless video monitoring and LAN connectivity [2]. Nowadays, FSO is getting the attention of 5G developers due to the large and unlicensed bandwidths available in the optical spectrum. Specifically, FSO has been proposed as a new physical layer technique for backhauling over small-to-medium distances (up to about 1 km), as long as line-of-sight can be guaranteed [3].

Propagation impairments are the biggest challenge for FSO. It is well known that fog, rain, snow, and turbulence produce significant signal fades even across short terrestrial FSO links [4], [5], [6], [7], [8]. Specifically, the severe propagation loss caused by fog reduces the availability of terrestrial optical links, where fog occurrence is statistically relevant. Hence propagation puts a practical limit on the maximum path length if high-availability standards are required. Similarly, mmWave propagation is hampered by rain [9]. Due to their different sensitivity to fog and rain, FSO and mmWave can be seen as either alternative or complementary technologies. Hybrid FSO/mmWave systems that backup each other depending on the actual weather conditions have been proposed to maximize availability [10]. In respect to propagation through fog, the optical channel is wavelength sensitive. In this regard, most of current FSO systems work in the 1.550 μm window due to its compliance with eye-safety regulations [11] and the relative low cost of the hardware. However, following the development of quantum cascade laser sources and detectors [12], [13] in the 10 μm band, there is a growing interest in the longer wavelengths [14], where fog attenuation is, in principle, less challenging.

In view of a possible deployment of FSO in mobile networks, there is a demand for simple and global channel models. Differently from the well-settled ITU-R recommendations containing methods for the prediction of propagation impairments at microwaves and mmWaves [15], there is a lack of standardization in the frame of FSO. ITU-R P.1817.1, entitled "Propagation data required for the design of terrestrial free-space optical links" includes only general guidelines and it has not been updated for a while [16]. This paper aims at filling gaps in the modelling and quantification of the path loss component due to fog.

There is a proliferation of models, which predict the extinction coefficient γ (i.e., the path loss across a unit path length) at different optical wavelengths from measurements of the visibility (V) [17], [18], [19], [20], [21] or of other atmospheric parameters [22], [23]. In this paper we adopted the approach based on V, because historical time series of visibility have been collected in many locations around the world over a long time for aviation safety and meteorological purposes. However, there are a number of issues that need investigation. First, visibility must be defined in quantitative terms as visibility measurements are carried out by different methods (e.g., through automatic sensors or human observations) [24], which have different accuracies. This aspect is addressed in Sections II.A and II.B. Moreover, some available models rely on rather old measurement datasets or on a limited sample of fog types. A survey of the available $\gamma - V$ models is in Section II.C. The analytical approach in Section III outlines the sensitivity of γ to the microphysics by calculating the optical properties of a large set of fog types, including recent data, which highlight differences with respect to older ones. In Section IV, we discuss some important limitations

Manuscript received November 11, 2021; revised January 28, 2022; accepted February 12, 2022. Date of publication February 22, 2022; date of current version March 24, 2022. This work was supported by the Coordenação de Aperfeiçoamento de Pessoal de Nível Superior - Brazil. *(Corresponding author: R. Nebuloni.)*

R. Nebuloni is with the Istituto di Elettronica e di Ingegneria dell'Informazione e delle Telecomunicazioni del Consiglio Nazionale delle Ricerche, 20133 Milan, Italy (e-mail: roberto.nebuloni@ieiit.cnr.it).

E. Verdugo is with the Departamento de Engenharia Elétrica of Pontifícia Universidade Católica do Rio de Janeiro, Rio de Janeiro 22451-900, Brazil (e-mail: elizabethverdugo@aluno.puc-rio.br).

Digital Object Identifier 10.1109/JPHOT.2022.3152728

of the modelling approach based on the visibility, whereas, in Section V we quantify the effect of model uncertainties on FSO link budget and we address some other system aspects. Finally, the conclusions are drawn in Section VI.

II. Propagation Models Through Fog

Based on an extensive analysis of surface observations made available online by Wyoming University [25], we concluded that the visibility value exceeded for 99.9% of time in most European cities ranges from less than 100 m to about 2 km. This effect is mostly due to fog, as rain reduces the visibility below a few km during a much smaller percentage of time. On the other side, in different climates, where fog is relatively infrequent, heavy rain may have a significant impact on the statistical distribution of optical attenuation. In this case, a propagation model based on the rainfall rate rather than on visibility statistics can be adopted [26]. Let us assume that FSO availability is driven by fog occurrence. Moreover, we suppose that 1) multiple scattering effects are negligible, and 2) the actual attenuation across a path L is given by $\gamma \times L$. The above two assumptions will be discussed in Section IV.

The $\gamma - V$ models proposed in the literature rely mainly on two approaches:

I) Microphysics of fog and electromagnetic theory.
II) Empirical derivation from joint measurements of optical attenuation and visibility.

In principle, the extinction coefficient of an optical wave travelling through any atmospheric particulate (fog, haze, rain, snow, etc.) can be accurately calculated from the particle size distribution (PSD) and the extinction cross section of a particle of given size [27]. The microphysical model highlights the sensitivity of wave attenuation to the radiation wavelength and to the PSD shape. However, it is not suitable for assessing the climatologic (i.e., long-term) distribution of attenuation required by link budget calculations as microphysical data are often unknown. Moreover, they change over different space and time scales (e.g., environment, climatic area, event life cycle, season). On the other side, empirical models based on different atmospheric parameters have been developed to predict optical attenuation. Here, we consider simple models using visibility as the only input. Visibility is routinely collected at many airports throughout the world, hence this approach may help in setting-up a global model to predict the component of optical attenuation due to fog.

A. $\gamma - V$ Relationship

A quick survey of the literature highlights a certain degree of scatter among different $\gamma - V$ models, which depends on the methodology followed in their derivation as well as on the definition of visibility. First of all, the visibility must be defined according to an objective rule. Following WMO recommendations [28], the visibility is equivalent to the meteorological optical range (MOR), i.e., the atmospheric path length required to reduce the irradiance (i.e., the optical power per unit area) of a perfectly collimated beam from an incandescent lamp at a colour temperature of 2700 K, to 0.05 times its value at the transmitter aperture. By means of the Bouguer-Lambert law, which predicts an exponential decay of the irradiance for propagation through a uniform layer of particles, it is straightforward to retrieve the following relationship between γ (in dB/km) and V (in km):

$$\gamma = \frac{13}{V} \tag{1}$$

Instrumental methods often make use of (1) to derive V from measurements of γ within a sample volume of the atmosphere. Sometimes, a different threshold value T for the irradiance is used, hence, for convenience, let us write (1) in a more general way as

$$\gamma = \frac{K}{V}\,, \tag{2}$$

where

$$K = -4.34 \ln T \tag{3}$$

Even though actual visibility sensors generally follow WMO recommendations and return the MOR, the majority of $\gamma - V$ models used in FSO applications adopt $T = 0.02$ (for the reasons detailed below), hence $K = 17$. Please note that (2) is just a definition, it holds in the visible part of the optical spectrum ($0.400 - 0.700\,\mu\mathrm{m}$), and it descends from the concept of MOR, which, in turn, quantifies the power loss of a collimated beam of given characteristics, as it travels through the atmosphere. Therefore, if the atmosphere is homogenous across a path L and multiple scattering is negligible, V is inversely proportional to the extinction coefficient of the visible radiation.

B. Visibility Measurements

As visibility has usually been (and it is still being) measured by human observers, the MOR should be linked to the intuitive definition of visibility that is, the maximum distance at which an object can be seen and recognized (at daytime) against the background[1]. This step can be done through the concept of irradiance contrast, which is the ratio of the difference between the irradiance of an object and the one of its background to the irradiance of the background itself. Hence, if the visibility (strictly speaking, the visual range) is now the distance at which the contrast of the observed object equals the contrast threshold of the observer, then the $\gamma - V$ formula can be written as in (2), where, now, T is the contrast threshold value [28]. The derivation of (2) from the contrast is due to Koschmieder [29], who proposed $T = 0.02$, hence $K = 17$, which is often reported instead of (1). Indeed, (2) with $K = 17$ has been incorporated by several $\gamma - V$ models, as the relationship in force at $\lambda = 0.550\,\mu\mathrm{m}$. Pierce *et al.* [30] reviewed the assumptions behind Koschmieder derivation. They provided a definition of the contrast in foggy and hazy atmosphere that accounts for light scattering from the suspended particles as well as for the effect of other light sources. The above two factors concur in reducing the contrast, hence, visibility measurements contaminated by scattering and background radiation may produce an overestimate of optical attenuation if Koschmieder

[1]This definition is more general than the one in [28], where visibility (at daytime) is the maximum distance at which a black object can be distinguished against the sky horizon.

TABLE I
RECOMMENDED VALUE OF THE COEFFICIENT K IN (2)

K	Measurement method	Uncertainty (std. dev.)
9.6	Visual observation of a light source at night	40%
11.3	Visual observation of a black object against the sky horizon during day	22%
13.0	Instrumental measurement of the MOR defined as in Section II.A	5 – 20%
$-4.34 \ln T$	Instrumental measurement of the visibility defined as the distance where the irradiance of a light source reduces to a fraction T of its value close to the source.	

formula is used. The authors came up with the main conclusion that optical attenuation can still be estimated by (2) and provided an interval of values for the coefficient K ($8.5 \leq K \leq 17$) rather than an optimum value. They indicated Koschmieder's value as a reasonable upper bound, and concluded that the actual value of K should be determined experimentally.

Visibility measurements based on the contrast of a distant object are carried out by the naked eye in many cases or, sometimes, by a CCD camera [31], [32]. In the former case, the contrast threshold is subjective, which generates further uncertainty in linking visibility measurements to the MOR, hence to the extinction coefficient. According to [28], visual estimates of visibility during daylight are about 15% higher than instrumental measurements of MOR (i.e., $K = 11.3$) with a 22% standard deviation, assuming a Gaussian distribution of the uncertainty. Visual observations at night-time are even more problematic, as they require a light source of known intensity and depend on factors as the background illumination. Human observer's estimates of night-time visibility are 30% higher than MOR ($K = 9.6$), with an uncertainty up to 40%. On the other side, the accuracy of visibility sensors is usually provided by the manufacturer in datasheets and it is typically between 5% and 20% [24]. Another source of uncertainty is in the way visibility data are stored in the databases of public domain. Sometimes the meteorological reports make available numerical codes instead of visibility values. For instance, SYNOP VV codes for horizontal visibility at surface are integer values ranging from 00 to 99 [33] and have an accuracy within 100 m for visibility up to 5 km. This means that a 500 m visibility value is affected by a 20% quantization error. Visibility data encoding is even coarser at times. Please note that, by virtue of (2), the percent uncertainty over γ equals the one over V. Table I summarizes the recommended relationships to convert visibility into extinction coefficient in the visible window as well as the associated uncertainties.

C. Wavelength Dependence

Equation (2) strictly holds in the visible region of the spectrum. Actual FSO systems work in the near–IR spectral windows where the atmosphere is transparent, i.e., 0.780–0.950 μm, or, more often around 1.550 μm where they take advantage of low-cost and well-consolidated optical fiber technology. Nowadays, mid-IR systems operating around 10.6 μm are attracting some interest due to the development and improving performances of quantum cascade laser sources and detectors [12]. The wavelength dependence of the $\gamma - V$ relationship can be accounted by a power-law function, which fits the asymptotic regime of Rayleigh scattering as well. We move from the following formulation that is common to a number of models:

$$\gamma = \frac{K}{V} \left(\frac{0.550}{\lambda} \right)^q \tag{4}$$

where λ is in μm and q depends on V. A few expressions have been proposed for q [17], [18], [19]. The following Table II lists a number of models available in the open literature. Some of them are best-fits of optical propagation data collected through fog and haze, whereas some others descend from scattering calculations using known analytical expressions for the PSD. One of the most recurrent models is the one in Kruse textbook [18], which is sometimes referred to as Kruse model even though it is largely based on earlier works. Several authors pointed out that this model is not appropriate for fog, hence the expression of q for $V < 6$ km in Table II should not be used for propagation through fog. Kim *et al.* [17] proposed different values for q based on existing literature, even though they did not provide any evidence of their findings. They just stated that "*in haze conditions, there is a wavelength dependence to the atmospheric attenuation. However, it has been shown through an extensive literature search of past experimental observations and some full Mie theory scattering calculations, that this is not the case in fog*". Specifically, they broke the 0 - 6 km visibility interval into three segments and suggested to take $q = 0$, if $V < 500$ m. This fact has deep implications as it means that in dense fog, optical attenuation is independent of the wavelength, at least up to 1.550 μm, as the authors limited their analysis to the visible and near-IR domains. On the other side, if $V > 500$ m, [17] predicts a significant improvement of optical transmission in the 1.550 μm window over shorter wavelengths with increasing visibility. For instance, $\gamma_{1.550}$ reduces by 40% if $V = 1$ km with respect to γ_{vis} and by 30% with respect to $\gamma_{0.785}$, respectively.

Two relationships based on Mie scattering theory and analytical models of the PSD of fog are reported as well in Table II. Grabner and Kvicera [20] used a three-parameter gamma function to describe the PSD of fog, introducing constraints to reduce the number of free parameters. Their $\gamma - V$ formulation is as in (4). However, the expression for q is rather complicated and wavelength-dependant, because γ does not exhibit a monotonic decrease with increasing λ in the interval considered by the authors (0.2–2 μm). Their $\gamma - V$ curve is convex on log-log axes and, contrary to [17], it predicts larger γ values than (2) in the near-IR rather than in the visible range and at 1.550 rather than at 0.785 μm. The increase of γ above the value at 0.550 μm is within 10% at 0.785 μm if $V \leq 2$ km, while it is a remarkable 35% at 1.550 μm in the interval 1–2 km. Al Naboulsi *et al.* [21] calculated best fit expressions for γ of radiation fog and heavy advection fog models tabulated in [34], in the wavelength interval 0.69–1.55 μm. Wavelength dependence is rather weak, because the dominant particle size

TABLE II
LIST OF $\gamma - V$ MODELS. V IS IN km, γ IS IN db/km, AND λ IS THE WAVELENGTH IN μm

ID	MODEL NAME	Model	Comment
1	Definition of visibility	$\gamma = \frac{K}{V}$	If *K=13*, *V* equals the meteorological optical range (MOR) [28].
2	Kruse [18]	$\gamma = \frac{17}{V}\left(\frac{0.550}{\lambda}\right)^q$, $q = \begin{cases} 1.6 & V > 50 \text{ km} \\ 1.3 & 6 \text{ km} < V < 50 \text{ km} \\ 0.585V^{\frac{1}{3}} & V < 6 \text{ km} \end{cases}$	
3	Kim [17]	$\gamma = \frac{17}{V}\left(\frac{0.550}{\lambda}\right)^q$, $q = \begin{cases} 1.6 & V > 50 \text{ km} \\ 1.3 & 6 \text{ km} < V \leq 50 \text{ km} \\ 0.16V + 0.34 & 1 \text{ km} \leq V \leq 6 \text{ km} \\ V - 0.5 & 0.5 \text{ km} \leq V < 1 \text{ km} \\ 0 & V < 0.5 \text{ km} \end{cases}$ $0.400\ \mu\text{m} \leq \lambda \leq 1.55\ \mu\text{m}$	Kruse model upgrade for fog conditions.
4	Grabner [20]	$\gamma = \frac{K}{V}\left(\frac{0.550}{\lambda}\right)^q$, $q = -2\left(\tanh\left(p_1(w + p_4)\right) - 1\right) + p_2 \exp(-p_3(w + p_5)^2)$, $w = \log_{10} r_e$, $r_e = 10\sqrt{\frac{0.05}{V}}$	Microphysical model. Based on fog PSD modelling by the gamma function.
		Coefficient: $0.2 < \lambda < 0.55\ \mu$m: p_1 2.21888, p_2 0.67214, p_3 8.04794, p_4 0.8, p_5 0.3; $0.55 \leq \lambda < 2\ \mu$m: p_1 1.94311, p_2 0.59076, p_3 6.36656, p_4 0.45, p_5 -0.15	
		$0.2\ \mu\text{m} < \lambda < 2\ \mu\text{m}, V \leq 10$ km	
5	Al Naboulsi [21]	$\gamma_{Adv} = \frac{0.49848\lambda + 16.66258}{V}$, $\gamma_{Rad} = \frac{0.78720\lambda^2 + 0.59537\lambda + 16.28691}{V}$ $0.690\ \mu\text{m} \leq \lambda \leq 1.55\ \mu\text{m}, 0.05 \text{ km} \leq V \leq 1$ km	Microphysical model for advection and radiation fog.
6	Nebuloni [19]	$\gamma = aV^b$	Best fit of measurements carried out by several authors.

Center	Center-band (μm)	Visibility (km)	Coefficient *a*	Coefficient *b*
Visible	0.55	$V > 0$	16.98	-1.00
Near IR	1.20	$0.06 \leq V < 0.5$	15.85	-1.02
		$0.5 \leq V < 2$	12.38	-1.38
Mid IR	3.70	$0.06 \leq V < 0.5$	13.07	-1.11
		$0.5 \leq V < 10$	10.42	-1.43
Far IR	10.6	$0.06 \leq V < 0.5$	5.30	-1.30
		$0.5 \leq V < 3$	2.30	-2.51

of the chosen PSDs (two modified gamma functions) is larger than the maximum wavelength in both cases (mode radius equal to 2 μm and 10 μm, respectively). Therefore, the departure of their $\gamma - V$ formula from (2) is modest.

Fig. 1 highlights the pattern of the predicted extinction coefficient at 1550 μm against the visibility according to the aforementioned models. For convenience, we used $K = 17$, as this value has been usually adopted in the models. Please note that, when a different value of K is used instead, (e.g., $K = 13$, if the visibility sensor measures the MOR), the corresponding threshold values on V in the table must be scaled accordingly. It descends that the important limit of 500 m in [17] changes to 650 m when expressed in terms of the MOR. In the next section, a large database of PSDs will be considered to assess the above models taking in due account the variability of fog.

III. THE MICROPHYSICAL MODEL

The microphysical model relies on the knowledge of the PSD. Measured particles are binned into size intervals and usually fitted with analytical curves. Finally, γ is calculated through the classical single-scattering integral. The extinction cross section σ_{ext} of fog droplets must be computed by Mie theory (assuming homogeneous and spherical water particles) as the droplet radius

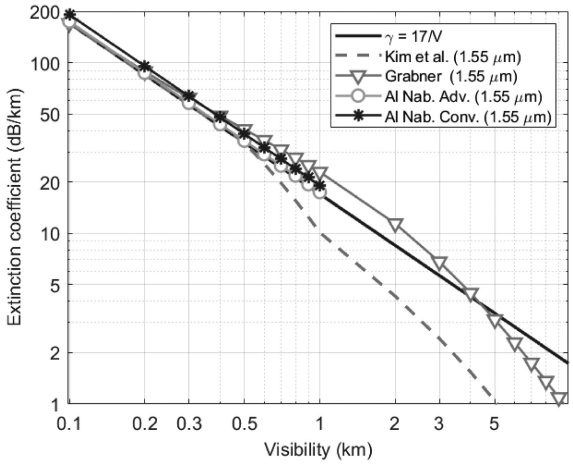

Fig. 1. Extinction coefficient at 1.55 μm against visibility according to different models. The relationship $\gamma = 17/V$ is the definition of visibility, which holds at 0.550 μm.

r is comparable with FSO wavelengths. The integral expression for the extinction coefficient is

$$\gamma\ (\lambda) = 4.34 \times 10^{-3} \int_{r_1}^{r_2} \sigma_{ext}\,(r, \lambda)\, N\,(r)\, \mathrm{d}r \qquad (5)$$

where $N(r)$ is the PSD expressed in $\mathrm{cm}^{-3}\mu\mathrm{m}^{-1}$, σ_{ext} is in $\mu\mathrm{m}^2$ and γ is in dB/km.

The two $\gamma - V$ models discussed in the previous section and based on microphysics highlight rather different γ values due to the different PSDs used by the authors. Here, fog microphysics is used to provide a theoretical validation of the $\gamma - V$ models as well as to get an insight on the relationship between V and γ at different wavelengths, following the approach in [8]. We use a larger database made of 54 PSDs of fog and haze, including recent measurements. Specifically, we take advantage of extensive observations of the PSD of radiation fogs in Paris by spectrometers in the particle range 0.2 to 50 μm [23]. These data highlight that fog is characterized by multimodal PSDs, modelled by as many lognormal functions. An overall 20 multimodal PSDs were reported in [23], corresponding to different stages of fog. The remaining 34 PSDs used in this paper are taken from older studies and were usually modelled by modified gamma distributions [34], [35], [36], [37].

Fig. 2(a) and (b) show the extinction coefficient at 1.550 and at 10.6 μm against the visibility, considering the above 54 PSDs. The 34 monomodal distributions are grouped by fog type. In the case of valley fog, the authors in [35], [37] further distinguished into four evolutionary stages (i.e., growth, formation, mature and dissipation fog), which are drawn with as many markers to highlight the dependence of $\gamma - V$ on the life cycle of fog. Moreover, all the monomodal distributions were tabulated for nominal values of the particle number concentration. Therefore, as in [8], the number concentration is considered a parameter and it is allowed to range within realistic limits, hence the corresponding PSDs are segments rather than points in the $\gamma - V$ plane of Fig. 2. On the other side, the actual number concentration was provided in [23] for the multimodal PSDs (filled circles). Equation (4) at 0.550 μm is drawn in Fig. 2(a)

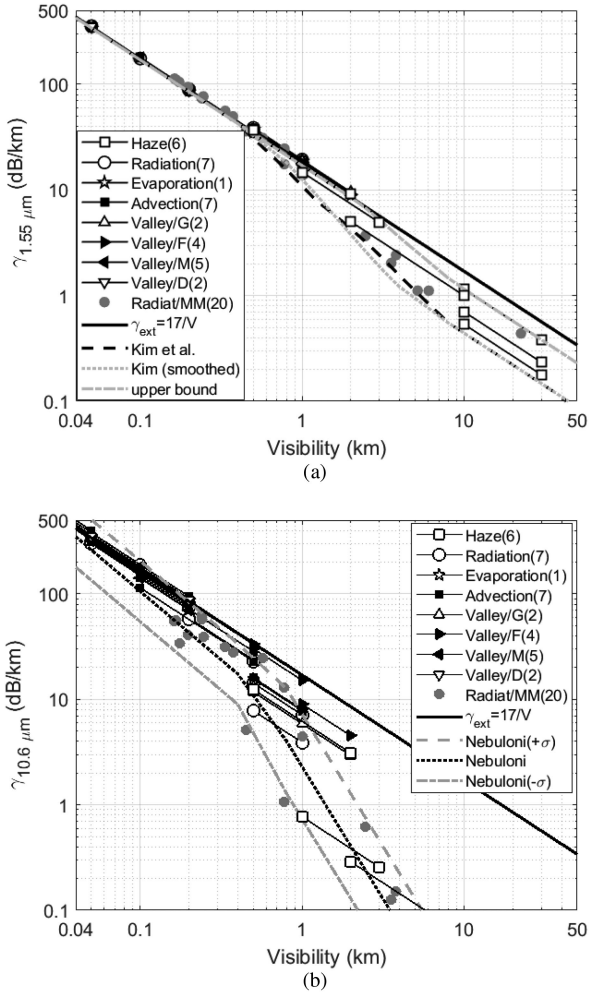

Fig. 2. Extinction coefficient against the visibility for 54 fog and haze types at (a) 1.550 μm, and (b) 10.6 μm. A few $\gamma - V$ models are shown as well and discussed in the text.

and (b) as well as a reference. Finally, Kim model (1.550 μm) and Nebuloni model (10.6 μm), taken from Table II, are plotted. Again, for consistency with original model formulations, we take $K = 17$. At 1.550 μm, γ is bounded by Kim model and by (4). The markers are packed around $\gamma = 17/V$ as far as V is less than about 1 km, whereas γ tends to decrease below $\gamma = 17/V$ as V increases. This trend is predicted by Kim model even though it provides a lower bound of PSD data rather than a satisfactory fit. On the other side, at 0.785 μm (not shown), there is no significant departure from (4) even at large visibility values. To summarize, fog attenuation is roughly wavelength-independent from the visible range throughout the near-IR up to 1.550 μm as far as $V < 1$ km. Beyond this limit, 1.550 μm propagation seems better, as highlighted by the multimodal PSDs corresponding to the early and late stages of radiation fog in Paris.

The picture changes moving into the mid-IR range. Data depart from $\gamma = 17/V$ at a much lower visibility than in the near-IR. Even though there is a huge scatter, the trend towards a significant decrease of γ with respect to near-IR wavelengths is evident. The multimodal radiation fog data highlight that

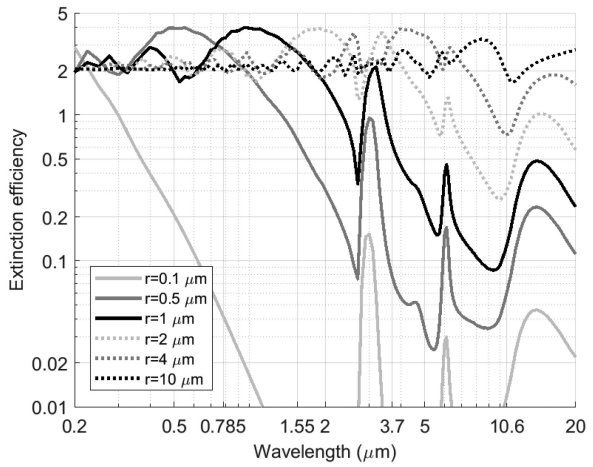

Fig. 3. Extinction efficiency of water droplets in the optical spectrum for six different droplet radii.

$\gamma_{10.6}$ can be significantly smaller than in the near-IR even in the presence of dense fog, which is not as evident looking at the monomodal PSDs. If V grows beyond about 200 m, 10.6 μm transmission is always better than at shorter wavelengths, the ratio of the corresponding extinction coefficients being up to one order of magnitude and even higher.

Fig. 3 provides a simple physical explanation of the above features by showing the extinction efficiency of water spheres as a function of the wavelength for different droplet radii. The efficiency is the ratio between σ_{ext} and the geometrical cross section of the particle. The extinction efficiency of water droplets is basically wavelength independent up to the near-IR range if $r \geq 4$ μm. At the same time, if $r \leq 4$ μm, the extinction efficiency in the 10.6 μm window decreases by a factor of 3 (at least) with respect to the near-IR, and by a factor of 10 for sub-micron particles. Of course, this is a simplified picture as real PSDs spread over a range of droplet sizes, which flattens the large variations highlighted in Fig. 3. What actually rules is the shape of the integrand function involved in the calculation of γ in (5), i.e., the product $\sigma_{ext}N$. However, the 4 μm threshold value is a relatively simple rule to bear in mind. For instance, the mode radius of the multimodal PSDs is much smaller (0.4 - 0.6 μm) than the one of the monomodal PSDs of radiation fog (2 - 12 μm), which explains the different features in the $\gamma - V$ plane.

There are two major conclusions from this section: first, in the near-IR, the departure from $\gamma = 17/V$ (or $\gamma = K/V$ if a different definition of visibility is used) is limited and it should be considered only at 1.550 μm when $V > 1$ km; second, in the mid-IR, the existing models are not adequate to describe the spread of $\gamma - V$. Fog attenuation at 10.6 μm can be much smaller than in the near-IR even in dense fog.

IV. Discussion

One core assumption of this paper is that fog microphysics, i.e., the PSD, and scattering theory provide a rigorous method for predicting the path loss (per unit length) due to fog. Given that 1) the dataset used here does not cover the full range of possible fog PSDs, and 2) the probability of occurrence of a certain PSD is unknown, the microphysical model does not have a practical application to FSO design. However, it is a useful tool to validate the simple $\gamma - V$ models. Moreover, when the microphysics has an impact, it makes sense to identify lower and upper bounds on γ, as visibility alone does not capture the complexity of the process. In the next section, limiting expressions for γ will be used to quantify the uncertainty of path loss estimation at system level. In the following, we discuss a few issues and limitations of the methodology proposed in Sections II and III.

Equation (2) is based on the Bouguer-Lambert law of exponential decay, which holds when multiple scattering effects are negligible. Multiple-scattering actually increases the number of photons impinging on the receiver, hence the received power. Its impact depends, among others, on the path length, on the wavelength and on the PSD. To quantify multiple-scattering effects through fog, we carried out simulations based on the approach used in [38]. Path attenuation decreases by less than 1% with respect to the simple calculation in (5) when we consider multimodal radiation fogs (visibility values of about 180 m) across a path length of 500 m. In the presence of heavy advection fog (visibility values down to 50 m), path attenuation decreases by 5% after 200 m. However, extremely low visibility values would produce link outage as practical FSO path lengths are few hundred meters at least. As a matter of fact, multiple-scattering corrections do not significantly affect the propagation loss through fog.

A limitation of the microphysical model, as well as of all models predicting the extinction coefficient, is the conversion into path attenuation across a path leng L. This is usually done by the simple scaling law γL. As a result of the inhomogeneous distribution of fog in space, path attenuation, on the average, will be less than the one estimated from visibility or PSD data sampled at a single-point. In this respect, visibility measurements collected by human observations of distant objects are better than automatic sensors, which usually carry out single-point measurements. However, to the authors' knowledge, there are not models available that include the above path reduction factor.

A different approach to validate $\gamma - V$ models and to evaluate the impact of the spatial distribution of fog relies on measurements of optical transmission and visibility. The latter can be measured by visibility sensors displaced along the link. Alternatively, path-averaged visibility values can be obtained from multi-wavelength transmission experiments featuring a laser in the visible range. A survey of older transmission measurements through fog is in [19]. Best fit curves and $\pm\sigma$ bounds were derived for the extinction coefficient at three different IR wavelengths (1.2, 3.7 and 10.6 μm) against the corresponding visibility values, obtained from data in the visible range. The best fit line at 1.2 μm (not shown) is close to Kim model. Data at 10.6 μm are scattered. However, the majority of fogs considered here are within the $\pm\sigma$ bounds calculated in [19] or close to them (see Fig. 2(b)). Possible issues with the results of [19] are that: 1) the dataset includes very different path lengths (from 17 m to 2.6 km), and 2) best fit lines at the three wavelengths are drawn from different datasets.

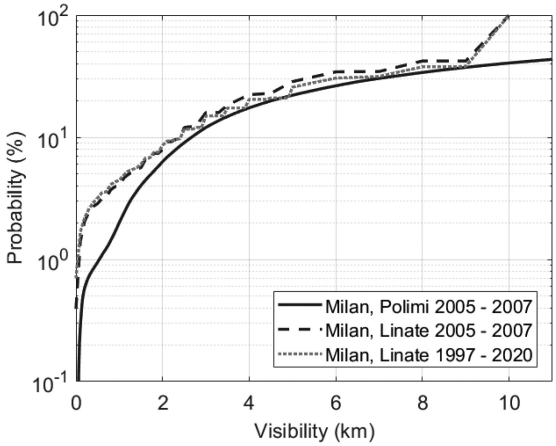

Fig. 4. Cumulative distribution function of the visibility measured in Milan in two different locations: Politecnico di Milano (urban area) and Linate airport (rural area).

Recent measurements in the first optical window indicate that $\gamma = K/V$, with $K = 13$ or $K = 17$, depending on the visibility sensor, fits the data fairly well, regardless of the environment and of the path length [39], [40], even though there are exceptions. The results at 1.550 μm are different and sometimes disagree to each other. For instance, the authors in [41] compared 1.550 μm measurements through radiation fog across a 85 m path with visibility data. The best fit of data is $\gamma \cong 10/V$ for V down to about 50 m (the authors did not specify the visibility range used to fit data though), against an expected $\gamma = 17/V$, at least when $V \leq 500$ m. The above trend was observed in 5 of the 6 events in their database. On the other side, transmission data at 1.550 μm and 0.532 μm during a moderate fog event (visibility down to 850 m according to the 2% rule) highlighted very similar path attenuation values [30]. Finally, the outcomes of experiments at 850 μm and 1.550 μm in [42] show larger γ values on both wavelengths than the ones predicted by the models if $0.3 \leq V \leq 1$ km. Specifically, $K = 20.6$ at 850 μm and $K = 18.2$ at 1.550 μm (visibility calculated by the 2% rule). There is a need for FSO field data featuring collocated visibility measurements and tests carried out over a significant number of events.

Another source of uncertainty for practical FSO design is that visibility measurements are not available in the location where FSO installation will take place. Indeed, fog is significantly affected by the microclimate. As an example, Fig. 4 highlights the difference between visibility records collected at Linate airport and at Politecnico di Milano campus (Italy). The airport is located in a rural area just outside the city borders and it is only 5 km away from Politecnico, which is into the city area. There are notable differences between the two cumulative distributions functions if visibility is less than 1 km. The probability that $V < 0.5$ km, 1 km and 2 km is three times, two times and 25% higher at Linate than at Politecnico. Even though these number are indicative, as measurements in Linate have a much coarser resolution in time and in space, the differences in visibility will reflect in a corresponding decrease of the optical extinction coefficient in the urban area for the same percentage of time.

V. FSO System Aspects

The path loss model enables to quantify fundamental FSO link design parameters as the maximum achievable path length. In the following, we evaluate the impact of $\gamma - V$ model inaccuracy on the calculation of the path length. In particular, we spotted two major sources of uncertainty in the conversion from visibility measurements to the extinction coefficient of fog, i.e.: 1) the way visibility is measured, and 2) the effect of fog microphysics. In the following, we assume that fog attenuation is the dominant component of the atmospheric path loss.

First, let us write a simplified FSO power budget equation [43]:

$$\gamma L - 10\log_{10}\frac{A_R}{\pi(\vartheta_T L)^2} + 60 = P_T - P_R - A_{sys} \quad (6)$$

where P_T and P_R are the transmitted and received power (in dBm), A_{sys} are system losses (dB), A_R is the receiver area (m^2), ϑ_T is the beam divergence (rad) and L is the path length (km), assuming homogenous propagation conditions across the path. The term on the right side of (6) depends on system characteristics. For the sake of simplicity, it is taken constant and hereafter named link margin M. The available link margin counteracts the sum of the path loss due to atmospheric attenuation (γL) and of the one due to geometric beam-spreading. Differentiating (6) leads to

$$\frac{dL}{L} = -\left[1 + \frac{20}{\ln 10}\frac{1}{\gamma L}\right]^{-1}\frac{d\gamma}{\gamma} \quad (7)$$

Last, we calculate the sensitivity of γ to V, for instance at 1.550 μm, using lower and upper bounds for γ. As Kim model has discontinuous derivatives at the edge points of each segment, we use a third-order polynomials between the low visibility segment, i.e., $V \leq 0.5$ km (basically, wavelength-independent and approximated by $\gamma = K/V$) and the high-visibility range, ($V \geq 6$ km), which fits well within the Rayleigh regime, where, again, the exponent q is constant. Hence

$$\gamma = \frac{p_1}{V^3} + \frac{p_2}{V^2} + \frac{p_3}{V} + p_4 \quad (8)$$

and, imposing the continuity of the derivatives, we get $p_1 = -4.417$, $p_2 = 17.783$, $p_3 = -1.144$, and $p_4 = 0.453$. The new curve, which works as a lower bound on γ, is plotted in previous Fig 2(a) and labelled as "Kim (smoothed)". Similarly, we identify an upper bound. Now, we use different visibility thresholds, to fit better the outcomes of the microphysical model. The wavelength independent segment goes up to $V = 2$ km, whereas the Rayleigh regime is made to start from $V = 10$ km ($q = 1.3$). The polynomials are now constrained to pass through the PSD point of Fig 2(b) with the maximum γ value at 10 km. The resulting coefficients are: $p_1 = -51.525$, $p_2 = 53.242$, $p_3 = 2.380$ and $p_4 = 0.429$.

Using, for instance, the upper bound model in (7), we get the following relationships between the differentials of λ and V:

$$\frac{d\gamma}{\gamma} = \begin{cases} -\frac{dV}{V} & V < 2 \text{ km},\ V > 10 \text{ km} \\ -\frac{3p_1+2p_2V+p_3V^2}{p_1+p_2V+p_3V^2}\frac{dV}{V} & 2 \text{ km} \leq V \leq 10 \text{ km} \end{cases} \quad (9)$$

Finally, by substituting (9) into (7), we obtain the uncertainty on path length.

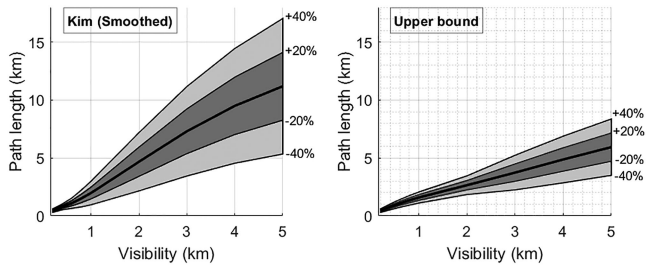

Fig. 5. Path length as a function of the visibility across the path (thick black lines) according to the smoothed Kim model and to the upper bound curve shown in previous Fig 2(a). Dark and light gray areas quantify the effect of visibility measurements affected by a relative uncertainty up to 20% and 40%, respectively.

Fig. 5 shows the achievable FSO path length at $1.550\ \mu$m as a function of the visibility across the link, according to the smoothed Kim model and to the upper bound model, respectively (thick black lines). Given V, γ descends from the chosen $\gamma - V$ relationship whereas the maximum achievable path length comes out of (6), once the other system parameters are specified. We used standard values of state-of-the art commercial FSO links, i.e., $\vartheta_T = 0.5$ mrad, $A = 0.01\ \mathrm{m}^2$ and $M = 50$ dB. The shaded areas represent the uncertainties due to the combined effect of the accuracy of visibility measurements and of the $\gamma - V$ model. The perimeters of the two shaded areas in gray correspond to 20% and 40% uncertainty bounds on V, respectively. For instance, if $V = 1$ km, and $dV = 0$, the path length value obtained with the smoothed Kim model is about $2V$, whereas it is $1.6V$ with the upper bound model (i.e., a 20% smaller). As far as the slope of the $\gamma - V$ curve is constant on log-log axes and, at the same time, atmospheric attenuation prevails over beam spreading loss, that is, if $V \leq 500$ m, then $\Delta L/L \cong \Delta V/V$ (replacing differentials by finite differences). Beyond this threshold, $\Delta L/L$ (in magnitude) slightly increases over $\Delta V/V$. In the worst case ($\Delta V/V = 40\%$), the combined effect of microphysics and visibility accuracy results in estimates of the path length, which differ by a factor close to three if $V = 1$ km and close to four if $V = 2$ km, respectively.

A basic link optimization process could be as follows. Suppose link performance is given in terms of availability, i.e., the percentage of time a target throughput is provided (with a certain BER). If the bandwidth and the modulation code are given, the above performance requirement turns into a requirement on the SNR. The latter is a bound on the minimum received power given the noise level. Moreover, if the FSO system characteristics in the power budget equation are known as well, the path loss due to the atmospheric channel determines a corresponding maximum achievable path length. Specifically, if cumulative distributions functions of visibility are available (as in Fig. 4), the procedure will be: convert V into γ, identify the value of γ corresponding to the required link availability, and, finally, derive the path length by the link budget equation. This approach assumes that the FSO propagation channel is characterized by visibility, at least for path loss modelling. A comprehensive channel model should include other sources of attenuation as clear-air scintillations, as well as address the temporal correlation of the channel. As for signal loss in clear-air, please note that turbulence and fog are, with good approximation, mutually exclusive. Hence, the full system margin against atmospheric losses is usually available to mitigate scintillations. Moreover, the actual FSO technology featuring direct detection significantly reduces scintillations by aperture averaging. For instance, with the parameter values in the above power budget example, the margin against atmospheric losses across a 1 km path would be about 30 dB. Given these numbers, clear-air turbulence is not expected to affect FSO link availability significantly, unless long links are employed [44]. Finally, the effect of the coherence time of the optical channel during fog or turbulent air motions is addressed in [45] and [46], respectively.

VI. Conclusion

Attenuation due to fog drives FSO power budget at least at mid-latitude and in continental climates. We investigated a simple model that predicts the extinction coefficient of fog γ from the visibility V. The majority of automatic visibility sensors rely on the meteorological definition of the visibility (MOR), which is proportional to the inverse of γ in the visible spectrum ($\gamma = K/V$). Fog attenuation is roughly wavelength independent at least up to 1.550 μm and visibility values up to 1 km. When V and/or the wavelength increase, γ drops below K/V, and, at the same time, it becomes less correlated with V, depending on fog type. In this respect, recent data of fog microphysics highlight multimodal PSD shapes, which, in turn, produce a more evident wavelength selective behavior than predicted by classical fog models. As a consequence, transmission in the 10.6 μm mid-IR window, can be significantly better than in the near-IR even in dense fog (i.e., $V << 1$ km). In general, it is recommended to identify bounds on γ (dependent on the visibility range of interest and on the wavelength), rather than using a best fit $\gamma - V$ line.

We investigated two types of uncertainties in the models based on V and their impact on FSO power budget. First, the accuracy of visibility data (and the $\gamma - V$ relationship) depends on the measurement method of V. Automatic sensors have standard deviations within 20%, while human observations are less accurate. Second, we assessed the effect of fog microphysics, identifying lower and upper bounds on γ, given V. At 1.550 μm, the $\gamma - V$ model uncertainty may result into a 20% error on the estimated path length of an FSO link if $V = 1$ km and into a 75% error if $V = 2$ km.

Visibility measurements are often collected just outside city areas (e.g., at airports) where fog is more frequent. The probability that $V < 1$ km within the city can be one half of the one in the surrounding rural area. Moreover, the spatial distribution of fog along the path is expected to reduce attenuation with respect to the numbers given here. Experimental set-ups featuring dual wavelength operation (i.e., near-IR and mid-IR) and a number of visibility sensors deployed across the path would help in assessing these effects.

REFERENCES

[1] M. A. Khalighi and M. Uysal, "Survey on free space optical communication: A communication theory perspective," *IEEE Commun. Surv. Tut.*, vol. 16, no. 4, pp. 2231–2258, Jun. 2014.

[2] T. Ismail, E. Leitgeb, and T. Plank, "Free space optic and mmWave communications: Technologies, challenges and applications," *IEICE Trans. Commun.*, vol. E99-B, no. 6, pp. 1243–1254, 2016.

[3] H. Tataria, M. Shafi, A. Molisch, M. Dohler, H. Sjoland, and F. Tufvesson, "6G Wireless systems: Vision, requirements, challenges, insights, and opportunities," *Proc. IEEE*, vol. 109, no. 7, pp. 1166–1199, Mar. 2021.

[4] M. S. Awan, L. Csurgai-Horváth, S. S. Muhammad, E. Leitgeb, F. Nadeem, and M. S. Khan, "Characterization of fog and snow attenuations for free-space optical propagation," *J. Commun.*, vol. 4, no. 8, pp. 533–545, 2009.

[5] V. Chimelis, "Extinction of CO_2 laser radiation by fog and rain," *Appl. Opt.*, vol. 21, no. 18, pp. 3367–3372, 1982.

[6] R. Nebuloni and C. Capsoni, "Laser attenuation by falling snow," in *Proc. 6th Int. Symp. Commun. Syst., Netw. Digit. Signal Process.*, 2008, pp. 265–269.

[7] D. K. Borah and D. G. Voelz, "Pointing error effects on free-space optical communication links in the presence of atmospheric turbulence," *J. Lightw. Technol.*, vol. 27, no. 18, pp. 3965–3973, 2009.

[8] R. Nebuloni and C. Capsoni, "Effects of adverse weather on free space optics," *Opt. Wireless Commun.*, pp. 47–68, 2016.

[9] F. Norouzian *et al.*, "Rain attenuation at millimeter wave and Low-thz frequencies," *IEEE Trans. Antennas Propag.*, vol. 68, no. 1, pp. 421–431, Sep. 2020.

[10] B. Bag, A. Das, I. Ansari, A. Prokes, C. Bose, and A. Chandra, "Performance analysis of hybrid FSO systems using FSO/RF-FSO link adaptation," *IEEE Photon. J.*, vol. 10, no. 3, May 2018, Art no. 7904417.

[11] "IEC 60825-1:2014 safety of laser products - Part 1: Equipment classification and requirements," IEC Standard 60825-1, 2014.

[12] J. Faist, F. Capasso, D. L. Sivco, C. Sirtori, A. L. Hutchinson, and A. Y. Cho, "Quantum cascade laser," *Science*, vol. 264, no. 5158, pp. 553–556, 1994.

[13] P. Corrigan, R. Martini, E. A. Whittaker, and C. Bethea, "Quantum cascade lasers and the kruse model in free space optical communication," *Opt. Exp.*, vol. 17, no. 6, pp. 4355–4359, 2009.

[14] E. Leitgeb *et al.*, "Analysis and evaluation of optimum wavelengths for free-space optical transceivers," in *Proc. 12th ICTON, IEEE*, 2010, pp. 1–7.

[15] *R. P. Propag. Data Prediction Methods Required Des. Terr. Line-of-Sight Syst.*, Recommendation ITU-R, 530–12, 2015.

[16] *R. P. Propag. Data Required Des. Terr. Free Space Opt. Links*, Recommendation ITU-R, 1817–1, 2012.

[17] I. I. Kim, B. McArthur, and E. Korevaar, "Comparison of laser beam propagation at 785 nm and 1550 nm in fog and haze for optical wireless communications," in *Proc. SPIE*, 2001, pp. 26–37.

[18] P. W. Kruse, L. D. McGlauchlin, and R. B. McQuistan, *Elements of Infrared Technology: Generation, Transmission and Detection*, New York, NY, USA: Wiley, 1962.

[19] R. Nebuloni, "Empirical relationships between extinction coefficient and visibility in fog," *Appl. Opt.*, vol. 44, no. 18, pp. 3795–3804, 2005.

[20] M. Grabner and V. Kvicera, "The wavelength dependent model of extinction in fog and haze for free space optical communication," *Opt. Exp.*, vol. 19, no. 4, pp. 3379–3386, 2011.

[21] M. Al Naboulsi, "Fog attenuation prediction for optical and infrared waves," *Opt. Eng.*, vol. 43, no. 2, pp. 319–329, 2004.

[22] P. Chylek, "Extinction and liquid water content of fogs and clouds," *J. Atmospheric Sci.*, vol. 35, no. 2, pp. 296–300, 1978.

[23] C. Klein and A. Dabas, "Relationship between optical extinction and liquid water content in fogs," *Atmos. Meas. Techn.*, vol. 7, no. 5, pp. 1277–1287, 2014.

[24] J. Crosby, "Visibility sensor accuracy: What's realistic. Symposium on meteorological observations and instrumentation," *Citeseer*, pp. 1–5, 2003.

[25] Global Surface Observations Dataset, Univ. of Wyoming, 2021. [Online]. Available: http://weather.uwyo.edu/surface/meteorogram/index.shtml

[26] U. Korai, L. Luini, and R. Nebuloni, "Model for the prediction of rain attenuation affecting free space optical links," *Electronics*, vol. 7, no. 12, pp. 407–420, 2018.

[27] H. C. Van de Hulst, *Light Scattering by Small Particles*, New York, NY, USA: Wiley, 1957.

[28] *Guide to Meteorological Instruments and Methods of Observation*, 8th ed., Geneva, Switzerland: WMO, 2018.

[29] H. Koschmieder, "Theory of horizontal visibility," *Contributions Phys. Free Atmos.*, pp. 33–53, 1924.

[30] R. Pierce, J. Ramaprasad, and E. Eisenberg, "Optical attenuation in fog and clouds," *Opt. Wireless Commun. IV*, vol. 4530, pp. 58–71, 2001.

[31] W. Wauben and M. Roth, "*Exploration of fog detection and visibility estimation from camera images*," presented at the WMO Tech. Conf. Meteorological Environ. Instruments Methods Observation (CIMO TECO), Madrid, Spain, Sep. 27–30, 2016.

[32] R. Babari, N. Hautière, E. Dumont, R. Brémond, and N. Paparoditis, "A model-driven approach to estimate atmospheric visibility with ordinary cameras," *Atmos. Environ.*, vol. 45, no. 30, pp. 5316–5324, 2011.

[33] *Manual on Codes - International Codes, Volume I.1, Annex II to the WMO Technical Regulations: part A- Alphanumeric Codes*, 2019. [Online]. Available: https://library.wmo.int/doc_num.php?explnum_id=10235

[34] E. P. Shettle, "Models of aerosols, clouds and precipitation for atmospheric propagation studies," in *AGARD Conf. Proc.*, Copenhagen, 1989.

[35] F. Tampieri and C. Tomasi, "Size distribution models of fog and cloud droplets in terms of the modified gamma function," *Tellus*, vol. 28, no. 4, pp. 333–347, 1976.

[36] D. Deirmendjian, "Far-infrared and submillimeter wave attenuation by clouds and rain," *J. Appl. Meteorol.*, vol. 14, no. 8, pp. 1584–1593, 1975.

[37] V. E. Zuev, "Atmospheric transparency in the visible and the infrared," Jerusalem, Israel: Israel Program for Scientific Translations, 1970.

[38] M. Grabner and V. Kvicera, "Multiple scattering in rain and fog on free-space optical links," *J. Lightw. Technol.*, vol. 32, no. 3, pp. 513–520, 2014.

[39] M. Gebhart *et al.*, "Measurement of light attenuation in dense fog conditions for FSO applications," *Atmos. Opt. Model., Meas., Simul.*, vol. 58691, pp. 175–186, 2005.

[40] K. Dev, R. Nebuloni, C. Capsoni, O. Fiser, and V. Brazda, "Estimation of optical attenuation in reduced visibility conditions in different environments across free space optics link," *IET Microw., Antennas Propag.*, vol. 11, no. 12, pp. 1708–1713, 2017.

[41] K. Fischer, M. Witiw, and E. Eisenberg, "Optical attenuation in fog at a wavelength of 1.55 micrometers," *Atmos. Res.*, vol. 87, no. 3/4, pp. 252–258, 2008.

[42] M. Grabner and V. Kvicera, "Physical and statistical modeling of attenuation due to atmospheric hydrometeors on free-space optical links at 850 and 1550 nm," in *Proc. SPIE*, vol. 8517, 2012.

[43] H. Manor and S. Arnon, "Performance of an optical wireless communication system as a function of wavelength," *Appl. Opt.*, vol. 42, no. 21, pp. 4285–4294, 2003.

[44] M.-A. Khalighi, N. Schwartz, N. Aitamer, and S. Bourennane, "Fading reduction by aperture averaging and spatial diversity in optical wireless systems," *J. Opt. Commun. Netw.*, vol. 1, no. 6, pp. 580–593, 2009.

[45] B. R. Strickland, M. J. Lavan, E. Woodbridge, and V. Chan, "Effects of fog on the bit-error rate of a free-space laser communication system," *Appl. Opt.*, vol. 38, no. 3, pp. 424–431, 1999.

[46] J. A. Anguita, M. A. Neifeld, B. Hildner, and B. Vasic, "Rateless coding on experimental temporally correlated FSO channels," *J. Lightw. Technol.*, vol. 28, no. 7, pp. 990–1002, 2010.